

# Act–Observe–Rewrite: Multimodal Coding Agents as In-Context Policy Learners for Robot Manipulation

Vaishak Kumar  
General Bionix, Inc.

**Abstract.** Can a multimodal language model learn to manipulate physical objects by reasoning about its own failures—without gradient updates, demonstrations, or reward engineering? We argue the answer is yes, under conditions we characterise precisely. We present **Act–Observe–Rewrite (AOR)**, a framework in which an LLM agent improves a robot manipulation policy by synthesising entirely new executable Python controller code between trials, guided by visual observations and structured episode outcomes. Unlike prior work that grounds LLMs in pre-defined skill libraries or uses code generation for one-shot plan synthesis, AOR makes the full low-level motor control implementation the unit of LLM reasoning, enabling the agent to change not just what the robot does, but how it does it. The central claim is that interpretable code as the policy representation creates a qualitatively different kind of in-context learning from opaque neural policies: the agent can *diagnose* systematic failures and *rewrite* their causes. We validate this across three robosuite manipulation tasks and report promising results, with the agent achieving high success rates without demonstrations, reward engineering, or gradient updates.

## 1. Introduction

Robot manipulation is entering an era of *foundation model integration*. Vision-language-action models trained on internet-scale data can generalise across hundreds of tasks zero-shot [3, 4]. Yet two significant challenges persist: (1) when these models fail on a specific deployment configuration, diagnosing *why* and adapting *without retraining* remains largely unsolved; and (2) the sheer cost of pretraining data and compute places such models out of reach for researchers who want to iterate quickly on novel manipulation tasks.

A complementary tradition has emerged in language agent research. Reflexion [24] showed that an LLM can improve performance on decision-making and programming tasks purely through verbal self-reflection—storing episode summaries in memory and using them as additional context in subsequent trials, with no weight updates. ReAct [32] demonstrated that interleaving reasoning traces with environment actions significantly outperforms imitation or RL baselines in grounded settings. Voyager [29] built an open-ended lifelong agent in Minecraft whose skill library grows entirely from LLM-generated executable code.

These results suggest a different paradigm for robot learning: instead of training a policy, *write* one—and *rewrite* it when it fails. The appeal is clear: no data collection, no training loops, full interpretability, and direct application of the LLM’s world knowledge about geometry, physics, and programming. The question is whether this paradigm is viable

for continuous physical manipulation, where success depends on precise kinematics, noisy vision, workspace geometry, and object physics—none of which admit the kind of clean natural-language characterisation that makes verbal reflection effective in text-based environments.

This paper addresses that question directly. We introduce **Act–Observe–Rewrite (AOR)**, a two-timescale framework: the robot executes an episode under a Python controller; between episodes, a multimodal LLM reasons over key-frame images and structured outcome data, diagnoses failure modes, and outputs an entirely new controller class. The new controller is dynamically compiled, validated, and loaded for the next trial.

The central claim of this paper is not a performance number. It is an *architectural claim*: that making the full controller implementation the unit of LLM reasoning—rather than a skill selector, a parameter vector, or a reward function—qualitatively changes what can be learned in-context. Specifically:

- The LLM can *diagnose the cause* of a failure in terms of code logic (“the y-coordinate is negated in the back-projection, which is wrong for OpenGL convention”), not just observe that failure occurred.
- The LLM can make *architectural changes*—adding phases, changing the target computation, introducing geometric corrections—that go far beyond parameter tuning.
- The LLM can reason about *physical constraints*—

workspace limits, sensor biases, grip geometry—and encode that reasoning as executable corrections.

**Contribution: The AOR framework:** a general architecture for code-synthesis reflexive learning in physical manipulation. Implemented with Claude Code as the coding agent, AOR achieves 100% on two tasks and 91% on a third. The experiments are reported honestly: the residual failures on Stack are an observed shortcoming—the agent identified gripper contact with the target cube as the cause but failed to discover a placement strategy that avoids it, even though one likely exists.

## 2. Background and Problem Formulation

### 2.1 The In-Context Policy Learning Problem

We consider a robot manipulation agent operating in episodic trials. At each timestep  $t$ , the agent observes images  $o_t$  and proprioceptive state  $s_t$ , and produces an action  $a_t \in \mathcal{A}$ . A trial terminates with outcome  $\tau = \{r, T, \phi_1, \dots, \phi_k\}$  where  $r$  is the scalar reward,  $T$  is the duration, and  $\phi_i$  are structured diagnostic signals (phase log, minimum distance to target, oscillation flag).

The *in-context policy learning problem* is: given the history of  $n$  past outcomes  $H_n = \{\tau_1, \dots, \tau_n\}$  and a set of key-frame images  $\mathcal{I}_n$ , produce an improved policy  $\pi_{n+1}$  without updating any model weights. Prior approaches differ in how they represent  $\pi$ :

- **Parameter update:**  $\pi$  is a fixed architecture; in-context improvement adjusts a parameter vector  $\theta$  [24].
- **Skill selection:**  $\pi$  selects from a fixed skill library  $\mathcal{S}$ ; in-context improvement changes the selection policy [1, 11].
- **Reward synthesis:**  $\pi$  is trained by RL; in-context improvement rewrites the reward function [16].
- **Code synthesis (AOR):**  $\pi$  is an executable Python class; in-context improvement rewrites the entire implementation.

The code synthesis approach is the most expressive: it can represent all of the above plus arbitrary algorithmic changes, new phases, and new geometric computations. Its risk is that the hypothesis space is so large that an LLM may produce incorrect or unsafe code. AOR addresses this with a compilation sandbox, action clamping, and a fallback to the previous working controller.

## 3. Related Work

### 3.1 Verbal Self-Reflection for Agents

Reflexion [24] is the closest antecedent to AOR. It introduced the principle of verbal reinforcement: after each trial, the agent produces a natural-language reflection stored in a

persistent memory buffer, which is prepended to the context for the next trial. Reflexion demonstrated 22% improvement on AlfWorld and 11% on HumanEval. However, Reflexion was designed for *text-based* environments (symbolic planning, code generation) where observations are structured and actions are discrete. The reflections modify *strategy descriptions* in natural language, not executable motor-control code.

AOR extends Reflexion to physical manipulation in three ways: (i) observations include raw RGB-D images requiring visual reasoning; (ii) the policy is executable motor-control code, not a language description; (iii) failure modes involve continuous kinematics and sensor geometry, not just logical errors. The key insight from Reflexion that AOR preserves and generalises is that *verbalising failure modes in natural language before rewriting policy is more effective than blind parameter search*.

Hong et al. [10] propose Reflective Test-Time Planning for embodied LLMs, combining reflection-in-action (pre-execution candidate generation), reflection-on-action (post-execution updates), and retrospective reflection (long-horizon credit assignment). Their work is the most direct embodied parallel to Reflexion and demonstrates strong improvements on long-horizon household tasks and MuJoCo environments. Feng et al. [8] extend this line with a VLM-based framework that imagines future world states to guide action selection across multi-stage manipulation tasks, outperforming MCTS and commercial VLMs on long-horizon benchmarks. **The key distinction from AOR** is the level of abstraction: both reflective planning approaches operate at the level of *sub-goal planning*—deciding which pre-built skill to invoke next—while AOR operates at the level of *skill implementation*, rewriting the motor-control code that executes a skill. The approaches are thus complementary rather than competing: one could use reflective planning for sub-goal selection while AOR handles low-level controller adaptation.

Self-Refine [18] generalises the reflection idea to arbitrary generation tasks: the same LLM produces output, critiques it, then refines it iteratively, improving code optimisation, maths, and dialogue quality. The generate–feedback–refine loop in AOR is structurally identical, but grounded in a physical domain: the “feedback” is visual and kinematic evidence from an episode rollout, not LLM self-critique, and the “output” is executable motor-control code, not free-form text.

ReAct [32] interleaved reasoning traces with environment interactions, achieving 34% absolute gains over RL/imitation baselines on AlfWorld with 1–2 in-context examples. AdaPlanner [26] added in-plan and out-of-plan revision strategies, reducing samples required by  $2\times$ . These works demonstrate strong in-context planning but, like Reflexion, operate in symbolic environments with discrete action spaces.

### 3.2 Code Generation for Robot Control

Code as Policies [15] demonstrated that an LLM can generate hierarchically structured robot control programs from natural language commands. Given a task description and a library of perception primitives, the LLM produces Python code that calls these primitives to implement the task. **The key distinction from AOR:** Code as Policies is *one-shot*—it generates code once and executes it. There is no closed-loop improvement from episode outcomes, no visual evidence of failure, and no iterative refinement. AOR adds the critical feedback loop: observe what happened, reason about why, rewrite.

ProgPrompt [25] used Pythonic program specifications to ground LLM task plans in available robot actions, achieving state-of-the-art on VirtualHome. Like Code as Policies, it is one-shot at the plan level, though the program representation is more structured.

SayPlan [21] and related works use LLMs to generate scene-graph-grounded plans from natural language. These approaches focus on *what to do* (task planning), not *how to do it* (motor-control implementation). AOR targets the latter.

ReKep [12] uses VLMs to express manipulation constraints as Python functions over tracked 3D keypoints, enabling zero-shot multi-stage and bimanual tasks from a single natural-language instruction. This is the closest prior work to AOR’s representation: both write Python code that reasons over visual observations at runtime. **The key distinction:** ReKep generates constraint code once from a scene description; it does not improve that code across episodes. AOR explicitly accumulates failure evidence across trials and rewrites the code in response, enabling systematic correction of errors that are invisible in a single observation.

### 3.3 LLM-Generated Reward Functions and Fitness Criteria

Eureka [16] used GPT-4 to generate reward function code, optimised over many RL training runs via an evolutionary outer loop, achieving human-expert-level reward design on 83% of 29 RL environments including dexterous tasks such as pen spinning. DrEureka [17] extended this to automate sim-to-real domain randomisation. Language to Rewards [33] translates natural-language task descriptions into reward function parameters for MuJoCo locomotion and manipulation controllers, bridging semantic instruction and low-level optimisation without manual reward engineering. RLCD [31] and related works use LLM feedback as a substitute for human reward labelling.

**The key distinction from AOR:** Eureka-style methods require many full RL training runs as the inner loop. Each outer-loop LLM call is followed by thousands of gradient updates. AOR requires only episode execution—each LLM call is followed by a single trial. This makes AOR substantially

cheaper and faster for rapid task adaptation, at the cost of lower peak performance on tasks that benefit from large-scale RL.

The two approaches are complementary: Eureka is optimal when RL training is feasible and the goal is maximum performance; AOR is optimal when fast adaptation and interpretability matter more than peak performance.

### 3.4 LLM-Based Optimisation

A growing body of work uses LLMs as black-box optimisers: rather than computing a gradient, the LLM is shown a history of (solution, score) pairs and asked to propose a better solution.

OPRO [30] formalised this idea directly: a meta-prompt contains past solutions sorted by score, and the LLM is asked to generate new candidates to maximise the objective. On prompt engineering and linear regression tasks OPRO matched or exceeded human-crafted solutions using only natural-language feedback. FunSearch [23] applied the same principle to combinatorial mathematics: an evolutionary outer loop selects high-scoring programs and feeds them back to the LLM as context, discovering new results in extremal graph theory and bin-packing. EvoPrompting [5] used LLMs to propose neural architecture mutations, combining evolutionary search with in-context program synthesis.

**AOR is an instance of LLM-based optimisation** where the objective is episode success rate, the solution space is Python controller code, and the “score” is a rich multimodal signal — key-frame images, reward traces, and phase-transition logs — rather than a scalar. The critical difference from OPRO and FunSearch is that AOR’s feedback is *visual and causal*: the LLM can see *where* the arm was at the moment of failure and reason about the physical cause, not merely observe that the score was low. This richer feedback enables targeted single-step improvements (e.g. fixing a sign error in the back-projection formula) that pure score-based optimisation would require many trials to discover by coincidence.

### 3.5 Grounded Planning with LLMs

SayCan [1] grounded high-level LLM planning with a learned value function scoring which robot skills are executable in the current scene. PaLM-SayCan achieved 74% execution success on long-horizon manipulation tasks. The key limitation is that SayCan requires pre-trained low-level skills; it cannot improve those skills through reflection.

Inner Monologue [11] continuously injected environment feedback as a running “inner monologue”—passive scene descriptions and success detection—into the LLM prompt, enabling closed-loop replanning. Inner Monologue improved on SayCan by allowing the LLM to detect and recover from execution failures, but its feedback is high-level (“the object was not grasped”), not diagnostic (“the arm descended 6 cm above the object because the depth centroid is on the visible surface,

not the centre”). AOR’s key contribution over Inner Monologue is the *depth* of diagnosis: by reasoning over images and controller code simultaneously, the LLM can pinpoint root causes at the level of individual lines of code.

GPT-4V for Robotics [28] uses multimodal LLMs to analyse human demonstration videos and synthesise robot programs. This is complementary to AOR: it provides a rich warm-start policy from demonstrations; AOR then refines it through self-improvement.

### 3.6 Foundation Models and VLAs for Manipulation

The dominant paradigm for generalised robot manipulation trains *vision-language-action (VLA) models* jointly on internet-scale data and robot trajectories. RT-2 [4] co-fine-tuned a large VLM on robot data, achieving emergent generalisation. PaLM-E [7] injected continuous sensor modalities into a 562B-parameter language model. OpenVLA [14] provided an open-source 7B-parameter alternative that outperforms RT-2-X (55B) by 16.5% with LoRA fine-tuning.  $\pi_0$  [3] combined a VLM backbone with a flow-matching action expert for dexterous manipulation. Octo [9] introduced the first open-source generalist policy trained on 800k episodes from Open X-Embodiment, supporting both language and goal-image conditioning with strong cross-embodiment transfer. The Open X-Embodiment [20] dataset and Gato [22] established the multi-task, multi-embodiment training paradigm. Most recently, dual-system architectures such as GR00T N1 [19] mirror cognitive fast/slow thinking: a slow VLM (System 2) reasons about instructions and scene context while a fast visuomotor policy (System 1) produces real-time actions. This two-system structure echoes AOR’s two-timescale design, but the timescale separation in GR00T N1 operates *within* a single inference pass, whereas AOR’s slow loop operates *between episodes*, accumulating experience to rewrite the fast controller.

**AOR occupies a fundamentally different position from VLA models** along several axes (Table 1). VLA models optimise for *breadth*: they generalise across hundreds of tasks through pretraining. AOR optimises for *depth and interpretability*: it achieves high performance on individual tasks through targeted reasoning, with a policy that can be read, audited, and modified by a human. The two are complementary: AOR-style reflection could provide targeted debugging when a VLA model fails on a specific deployment configuration without requiring full retraining.

Diffusion Policy [6] and ACT [34] represent the state of the art in data-driven visuomotor policy learning. Diffusion Policy outperforms prior methods by 46.9% on 12 tasks using multi-modal action distributions; ACT achieves 80–90% on bimanual tasks from 10 minutes of demonstrations. These establish an important comparison: *given demonstrations, data-driven methods outperform AOR*. The contribution of AOR is performance *without any demonstrations*.

### 3.7 In-Context Learning and Adaptation in Robotics

Instant Policy [27] demonstrated in-context imitation learning from 1–2 demonstrations via graph diffusion over scene graphs, enabling zero-shot generalisation to new tasks without weight updates. This is the closest gradient-free test-time adaptation baseline to AOR; the key distinction is that Instant Policy adapts to a *new task* from a demonstration, whereas AOR improves on the *same task* through its own failure history without any demonstrations.

RoboAgent [2] achieved generalisation across 38 tasks from 7,500 demonstrations by combining semantic augmentation with multi-task action-chunking. These approaches remain fundamentally demonstration-driven; AOR requires no demonstrations.

The approach most structurally similar to AOR at the code level is the concurrent work of Kagaya et al. on memory-augmented code adaptation [13], which maintains a library of successful control programs from prior environments and retrieves and adapts them as in-context examples for new settings. The key distinction is directionality: that work retrieves *successes* to prime new tasks, whereas AOR diagnoses *failures*—using visual keyframes as evidence—to iteratively correct the same task’s controller across episodes.

Closest in spirit to AOR otherwise is Eureka’s use of LLM-generated code with a feedback loop—but as argued above, the feedback loop in Eureka involves RL training, not episode-level trial and error. To our knowledge, AOR is the first system to demonstrate iterative *controller implementation* improvement for robot manipulation via LLM reflection over visual evidence, without any gradient updates.

## 4. The AOR Framework

AOR instantiates a two-timescale loop illustrated in Figure 1. The *fast loop* runs within an episode at control frequency; the *slow loop* runs between episodes at reasoning frequency. This decomposition is a deliberate design choice motivated by three considerations.

**Separation of concerns.** Physical control requires low-latency computation with deterministic timing guarantees. LLM inference is slow, expensive, and non-deterministic. Keeping the LLM strictly between episodes preserves real-time control properties while maximising the quality of the between-episode reasoning.

**Episode-level abstraction.** Single-timestep observations are too noisy for reliable LLM reasoning about manipulation failures. Episode-level summaries (phase logs, key frames, reward trajectories) abstract away within-episode noise and expose the systematic patterns that the LLM needs to reason about.

**Code as the interface.** The Python `Controller` class is a natural interface between LLM reasoning and robot execu-

Table 1: Comparison of AOR to related approaches along key dimensions. “Code unit” refers to whether the code generated is a full controller implementation, a reward function, a plan, or a skill-selection policy. “Failure-image FB” indicates whether the system uses visual key-frames from failed episodes as feedback.

Approach	Visual input	Code unit	Iterative	Failure-image FB	Zero-shot	Interpretable	Physical
Reflexion [24]	✗	Strategy	✓	✗	✓	✓	✗
Self-Refine [18]	✗	General	✓	✗	✓	✓	✗
Reflective TTP [10]	✓	Sub-goal	✓	✗	✓	Partial	✓
Code as Policies [15]	✗	Full plan	✗	✗	✓	✓	✓
ReKep [12]	✓	Constraint	✗	✗	✓	✓	✓
Eureka [16]	✗	Reward fn	✓	✗	✓	✓	✓
Inner Monologue [11]	✗	Skill select	✓	✗	✓	Partial	✓
Instant Policy [27]	✓	Action	✗	✗	✓	✗	✓
RT-2 / OpenVLA / Octo	✓	Action	✗	✗	✓	✗	✓
Diffusion Policy / ACT	✓	Action	✗	✗	✗	✗	✓
<b>AOR (this work)</b>	✓	<b>Full ctrl</b>	✓	✓	✓	✓	✓

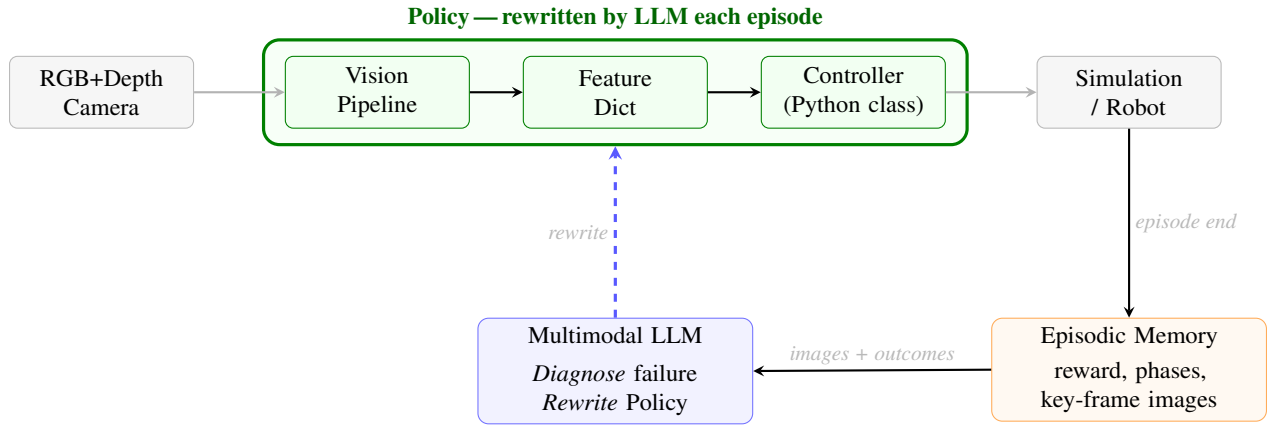


Figure 1: The AOR two-timescale loop. The **Policy** (green box)—comprising the vision pipeline, feature extraction, and Python controller—is the unit synthesised by the LLM after each episode. *Fast loop* (top): sensor observations flow through the Policy to produce actions each timestep, repeating at control frequency throughout an episode. *Slow loop* (bottom): at episode end, outcomes and key-frame images enter episodic memory; the multimodal LLM diagnoses failure modes and synthesises an entirely new Policy, dynamically compiled for the next trial. No model weights are updated at any point.

tion: it is human-readable (supporting diagnosis), machine-executable (supporting deployment), and compositionally modifiable (supporting targeted rewrites).

#### 4.1 The Four Components

**Vision pipeline:** Converts RGB-D images into a feature dict  $\mathbf{f}_t = \{\text{object\_pos}, \text{eef\_pos}, \text{detected}, \dots\}$  at each timestep. The vision pipeline is deliberately separate from the controller so that the LLM can reason about and rewrite them independently. The instantiation uses HSV colour-based segmentation, with the camera convention corrections described in Section 5.

**Controller:** A Python class with `reset()` and `get_action(features)` methods, safety-clamped

via a compilation sandbox. The controller can implement any strategy expressible in Python with NumPy: phase-based state machines, PID loops, waypoint sequences, geometric computations. This expressiveness is the key advantage of code synthesis over parameter-tuning or skill-selection approaches.

**Episodic memory:** Stores structured episode outcomes (reward, step count, phase-transition log, minimum EEF-to-object distance, oscillation flag) and a small set of key-frame images captured at phase transitions and at regular intervals. The memory is persistent across sessions.

**Multimodal LLM agent:** Receives the full memory context plus the current controller source code and produces a

new controller class. The agent is prompted to answer three questions before producing code: (1) What was the dominant failure mode? (2) Was the root cause in vision, controller logic, or parameters? (3) What is the single most impactful change? This structured reflection is directly inspired by Reflexion’s [24] verbal reinforcement principle but instantiated for code synthesis.

## 4.2 Safety and Stability Mechanisms

Several mechanisms prevent the code synthesis loop from producing unsafe or degenerate behaviour:

**Compilation sandbox.** All generated code is compiled and validated in an isolated namespace before execution. Any code that fails to compile, lacks the required interface, or raises exceptions at instantiation falls back to the previous working controller.

**Action clamping.** Every action returned by the controller is safety-clamped:  $[-2, 2]$  for Cartesian deltas,  $[-1, 1]$  for the gripper. Runtime exceptions per step produce a zero (safe-stop) action.

**Bounded rewrites.** The LLM is instructed to make targeted changes addressing the diagnosed failure mode, preserving the overall structure of the previous controller. Holistic rewrites that abandon all prior knowledge are discouraged. This is analogous to the bounded update principle in Reflexion.

## 5. Instantiation for Robot Manipulation

AOR is instantiated for the robosuite simulation platform. The key technical choices that implement the abstract framework described in Section 4 are presented here; experimental details follow in Section 6.

Importantly, the design choices described in this section were *not* prescribed by the authors. The agent was given only a task description, a robosuite environment, and a camera feed. Every architectural decision—the choice of colour segmentation over learned detection, the phase-based controller structure, the EMA smoothing scheme, the grasp-retry logic—emerged from the agent’s own iterative diagnosis and rewriting across episodes. The authors observed and recorded these decisions; they did not make them.

### 5.1 Vision Pipeline Design Choices

#### 5.1.1 Colour segmentation and the camera convention problem

For tasks with known-colour objects, the agent’s vision pipeline converged on HSV colour segmentation. A key insight discovered through AOR’s reflexive loop concerns *camera convention consistency*. Robosuite uses `IMAGE_CONVENTION = 'opencv1'`, meaning row 0 is at the image bottom and the camera uses  $y$ -up,  $z$ -back axes.

The correct pinhole back-projection is:

$$\mathbf{p}_{\text{cam}} = [x_p, y_p, -d, 1]^T, \quad x_p = \frac{(u-c_x)d}{f_x}, \quad y_p = \frac{(v-c_y)d}{f_y}. \quad (1)$$

The standard OpenCV formula uses  $-y_p$ , producing 5–8 cm errors. A further subtlety is that robosuite’s `get_camera_extrinsic_matrix` applies an OpenCV axis correction incompatible with OpenGL images; the world-to-camera transform must be computed directly from `cam_xmat`. These bugs are subtle, undocumented, and were autonomously discovered by the AOR reflexive loop—not by manual inspection (Section 6.2).

### 5.2 Controller Representation

The default controller template implements a sequential phase-based state machine: `reach`  $\rightarrow$  `descend`  $\rightarrow$  `grasp`  $\rightarrow$  `lift`  $\rightarrow$  {task-specific phases}. Phase transitions are threshold-based; each phase has a timeout fallback.

Two design principles emerged as invariant across all instantiations through the agent’s iterative reasoning:

**Stationary grasp.** During gripper closure, the EEF holds its position. Any downward pressing force destabilises the object. This is geometrically obvious but was not in the default controller; the LLM identified it as the root cause of grasp failure in the first Lift iteration.

**EMA smoothing.** Actions are smoothed via  $\mathbf{a}_t = \alpha \hat{\mathbf{a}}_t + (1-\alpha)\mathbf{a}_{t-1}$  with  $\alpha \in [0.3, 0.5]$ . The appropriate  $\alpha$  depends on object geometry: larger, more inertially stable objects tolerate higher  $\alpha$ ; lighter objects require higher smoothing to maintain grip integrity.

## 6. Experimental Validation

### 6.1 Setup

All experiments run on robosuite v1.5.1 under MuJoCo 3.2.3 with a UR5e arm and OSC\_POSE Cartesian delta controller. The coding agent is **Claude Code** (claude-sonnet-4-x family), Anthropic’s agentic coding assistant, which handles multimodal episode analysis and controller rewriting. All visual observations come from a single  $256 \times 256$  RGB-D `agentview` camera; ground-truth object positions are never used in the controller.

**Agent comparison:** We also ran the same three tasks using OpenAI’s Codex agent (GPT 5.3, High reasoning setting) as a direct substitute for Claude Code. The Codex agent was unable to solve any of the three tasks within the same iteration budget, failing to produce a working controller even for the simplest Lift task. This result highlights that agent capability is a meaningful variable in the AOR loop, and that the framework’s effectiveness is not independent of the underlying coding agent.

**Tasks:** Figure 2 shows the three tasks. We use three robosuite tasks of increasing complexity to test the claims in Section 4:

**Lift:** Pick up a red cube from a table surface. A diagnostic task designed to surface vision calibration requirements and validate systematic-failure rapid convergence. Success is unambiguous; failures produce informative phase logs.

**PickPlaceCan:** Pick up a cola can and place it into a designated bin. Tests whether AOR can resolve a systematic perception failure requiring correct colour identification and robust blob selection—specifically, the can renders as *red* (not silver) in the agentview camera, and the bin’s own red indicator marker must be suppressed.

**Stack:** Pick up a red cubeA and place it stacked on green cubeB. Requires two sequential visually-guided operations with  $\sim 2$  cm placement tolerance. The hardest task: exposes both systematic vision pipeline bugs and stochastic grasp dynamics, exercising multiple categories of the tractability taxonomy across 20 controller versions.

## 6.2 Experimental Observations by Failure Type

The experiments reveal a consistent pattern: AOR’s behaviour tracks the nature of the underlying failure mode. Evidence for each observed category follows.

**Systematic failures: rapid convergence** **Lift** converged to 100% in 3 LLM calls. Episode 0 failed entirely: the phase log showed `final_phase: reach` at 500/500 steps, indicating a systematic bias preventing descend. The LLM diagnosed a 2.5 cm vision depth bias and introduced a  $z$ -offset correction. Episode 1 reached grasp but failed: images showed the gripper flanking the cube and then the cube on the table—the LLM diagnosed downward pressing during closure as the root cause and changed to a stationary grasp. Episode 2 succeeded; 4/4 randomised repeats also succeeded.

**PickPlaceCan** converged to 100% in 2 LLM calls, each resolving one of two compounding perception bugs.

*Call 1 — wrong object colour.* Episode 0 showed the arm stalled in the reach phase for all 1000 steps. The LLM diagnosed a total detection failure: the initial `detect_silver_can` routine (low-saturation HSV mask) found no detections because the can renders as *red*, not metallic silver, in the agentview camera. The vision branch was rewritten to use a red-hue segmentor.

*Call 2 — bin indicator contamination.* With red detection active, Episode 1 showed the arm descending toward the *bin* side of the scene rather than the can on the table. The LLM diagnosed: `detect_red_object` averages all red pixels in the frame; the robosuite bin area contains a small red colour marker indicating the can’s target slot, whose pixels pull the centroid rightward. The fix was to switch to largest-connected-component filtering (`detect_red_can`), isolating the can—

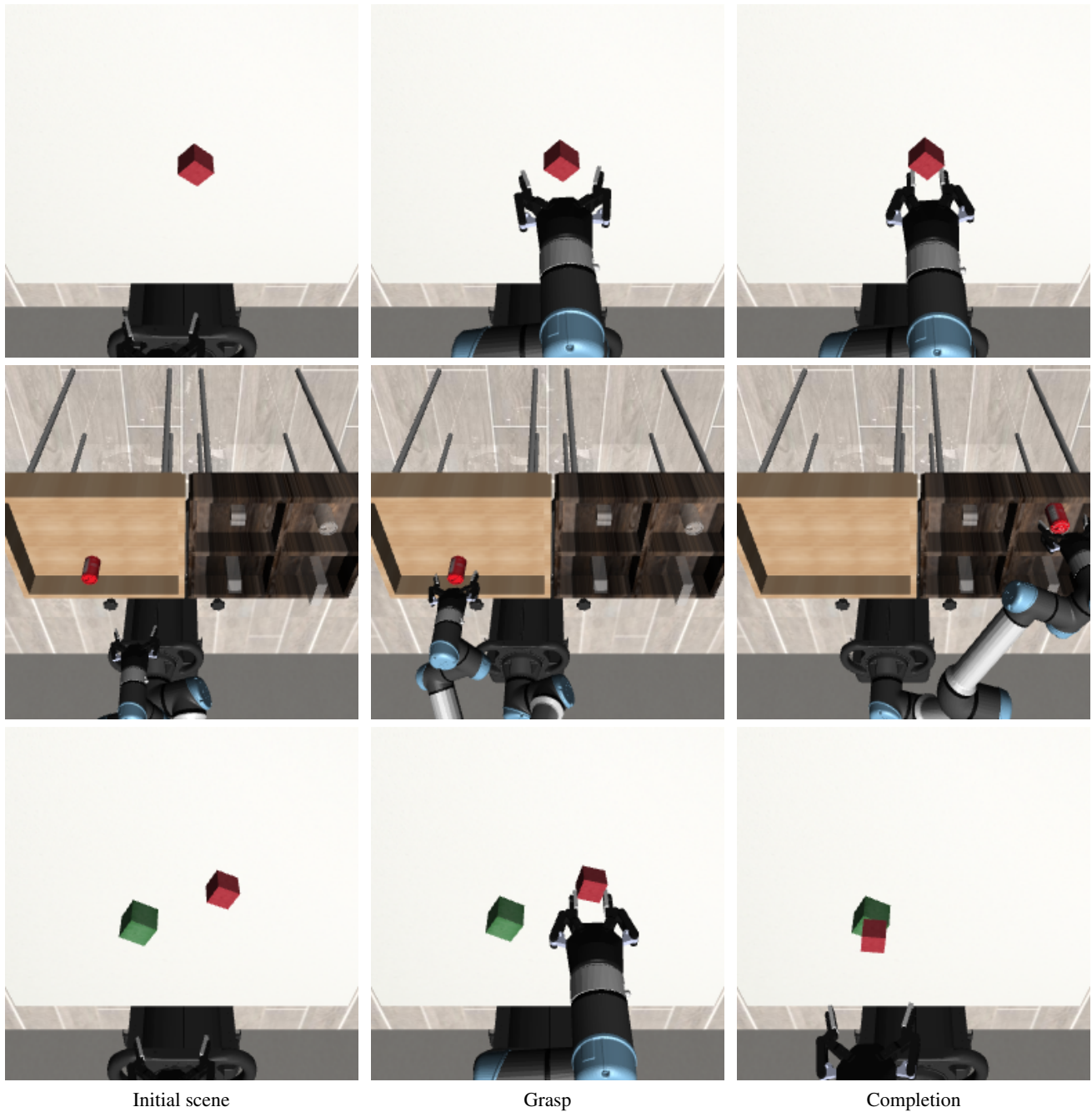


Figure 2: The three evaluation tasks, each shown at the initial scene, grasp, and task completion (all from the final controller version). *Top row: Lift* — pick up the red cube; converges to 100% in 3 LLM calls. *Middle row: PickPlaceCan* — grasp the cola can and drop it into the bin; achieves 100% after diagnosing the camera colour pipeline. *Bottom row: Stack* — pick up the red cube and place it on the green cube; reaches 91% after 20 controller versions addressing both vision pipeline bugs and stochastic grasp dynamics. All observations are from the  $256 \times 256$  agentview camera; no ground-truth object positions are used.

the largest red region— from the smaller bin indicator.

Episode 2 succeeded; 20/20 randomised repeats also succeeded, all without any simulator object-position readout.

**Stack (v0–v10)** exposed systematic vision pipeline bugs invisible at Lift’s precision tolerance but producing 5–8 cm errors at Stack’s 2 cm placement tolerance. After six controller iterations failed to improve placement precision, the LLM identified *vision inaccuracy* as the root cause. Two bugs were found: (i) back-projection with  $-y_p$  instead of  $+y_p$  (wrong for OpenGL convention); (ii) extrinsic matrix with an OpenCV axis correction incompatible with OpenGL images. Correcting both brought localisation errors to 1.4 cm (cubeA) / 1.9 cm (cubeB). Four further controller iterations reached 70% (Table 2).

Table 2: Stack controller progression. v0–v9 fix vision and control bugs; v17–v20 add grasp retries; residual failures are gripper–cubeB contact.

Version	Key change	Success
v0–v6	Controller tuning (vision error 5–8 cm)	0%
v7–v8	Back-projection y-flip fix	33%
v9	Extrinsic convention fix	45%
v10	Calibrated vision	70%
v11–v16	Retract ramp, descend tuning	~75%
v17	Grasp retry on failure	6/10
v18	Variable approach offset (buggy)	76%
v19	Separate offset per cube	83%
<b>v20</b>	<b>Freeze cubeB at place entry</b>	<b>91%</b>

**Observed shortcoming: failure to find a working placement strategy** The remaining 9% failure rate in Stack after v20 is not stochastic noise. Every failure episode completes the full phase sequence—grasp, lift, align, place, release, retract—but the stack does not hold. The cause is consistent and visible in episode images: the gripper fingers contact cubeB during the descent to place cubeA, physically displacing it before release.

The agent observed this correctly across failure episodes. After v20, the LLM’s reflection identified gripper contact with cubeB as the root cause. However, it did not discover a placement strategy that avoids the contact. Approaches such as a steeper descent angle, a compliant release from slightly above, or a lateral nudge-and-release likely exist and could resolve the issue—the agent did not explore them. The iteration terminated without a fix.

This is an honest shortcoming of the reflexion search as run in these experiments. The agent correctly diagnosed the failure but got stuck: it could not construct, within the hypothesis space it explored, a controller variant that places cubeA without disturbing cubeB. Whether a sufficiently capable agent or

a longer search would find the solution is an open question.

### 6.3 Overall Performance Summary

Table 3 summarises peak performance and iteration counts across all three tasks, annotated with the dominant failure type observed.

Table 3: Peak success rate and LLM-call count. Stack residual failures involve gripper contact with cubeB during placement; the agent diagnosed this but did not find a fix.

Task	Success	LLM calls	Residual failure
Lift	<b>100%</b>	3	None
PickPlaceCan	<b>100%</b>	2	None
Stack	<b>91%</b>	20	Gripper contact (unresolved)

## 7. Discussion

### 7.1 Code as the Right Representation for Reflective Learning

The central question of this paper was whether making the full controller implementation the unit of LLM reasoning qualitatively changes in-context learning in physical manipulation. The evidence says yes.

Consider the Stack task vision bugs. In a parameter-tuning framework (Reflexion-style), the LLM would observe that placement precision is poor and reduce thresholds or adjust gains. These adjustments cannot fix a sign error in the back-projection formula. In a skill-selection framework (SayCan, Inner Monologue), the skill implementations are fixed; the LLM cannot reach into them. In Code as Policies, there is no feedback loop to trigger re-examination. Only a code-synthesis framework with a closed loop and diagnostic prompts can identify “the y-coordinate in the back-projection has the wrong sign” and rewrite it. This is a fundamental capability advantage, not just a quantitative improvement.

The colour-pipeline diagnosis in PickPlaceCan makes the same point: the episode log showed the arm stuck in the reach phase for all 1000 steps, indicating a total detection failure. Recognising that the can rendered as *red* rather than silver, and that averaging all red pixels produced a centroid biased toward the bin’s colour marker, required understanding what the segmentor was computing and why. No parameter tuning or skill selection can express this; it requires rewriting the object-localisation logic.

### 7.2 Autonomous Perception Debugging

The autonomous discovery of the camera convention bugs deserves explicit discussion, as it illustrates a form of debugging absent from conventional robot learning. In standard imitation or RL pipelines, vision bugs are invisible: the policy simply fails to train to high performance, and the attribution

to vision vs. controller is unclear.

In AOR, the LLM has access to both the observation data (images showing where the arm went) and the implementation code (the back-projection formula). After Stack iteration 6, the LLM produced a diagnosis of the form: “the controller changes have improved convergence speed but the placement is consistently wrong by 5–8 cm—this is larger than any achievable parameter-tuning effect and the magnitude is consistent with a systematic back-projection error.” This level of attribution—from symptom to code module to specific line—is only possible because the LLM can read and reason about the code implementation.

This suggests that code-synthesis reflexive agents may be useful not just as policy learners but as *debugging tools* for any vision-based robot system, even ones that ultimately use learned policies.

### 7.3 Comparison to the Reflexion Family

The most precise comparison is with Reflexion [24] and Reflective Test-Time Planning [10]. All three operate in the in-context improvement paradigm; the differences are architectural.

Reflexion modifies *verbal strategies*, which are then interpreted by a high-level LLM producing discrete actions. This is effective in symbolic environments but cannot produce the geometric computations (back-projection correction, bin geometry target correction) needed for precise manipulation.

Reflective Test-Time Planning [10] operates at the sub-goal level: it decides which pre-built primitive to invoke next and how to adapt the plan when a sub-goal fails. The primitives themselves are fixed. AOR is complementary: one could use Reflective Test-Time Planning to select *which task to execute* while AOR learns *how to execute it*.

The generalisable principle emerging from all three works is: *in-context improvement is effective when the level of abstraction at which the LLM operates matches the level at which failures occur*. Reflexion matches text-level planning failures; Reflective TTP matches sub-goal-level failures; AOR matches motor-control implementation failures.

## 8. Limitations and Future Work

**Simulation only.** All results are from simulation. Real robots introduce sensing noise, actuation imprecision, and lighting variation that would require tighter uncertainty modelling. The techniques the agent introduced (colour-based segmentation, camera convention correction, grasp-retry mechanisms) are motivated by physical principles and should transfer to real hardware.

**Sequential iteration.** Each hypothesis is tested one trial at a time. Parallel hypothesis testing—generating multiple candidate controllers and evaluating them simultaneously—

would reduce wall-clock time substantially.

**LLM-dependence.** The quality of diagnosis depends on the LLM’s capability to reason about geometry, code, and physics. As LLMs improve, AOR performance is expected to improve without any changes to the framework.

**Incomplete search.** The Stack experiments reveal a shortcoming of the reflexion search: the agent correctly identified gripper contact with the target cube as the cause of residual failures but exhausted its iteration budget without finding a placement strategy to avoid it. The agent converged to a local optimum in controller space. Mechanisms such as explicit diversity pressure, restarts, or structured exploration of placement strategies are not present in the current AOR loop and would be needed to overcome this kind of search failure.

**Classical controller bias.** Left unprompted, the agent converged on classical control techniques—HSV segmentation, phase-based state machines, PID-style gains—because these are well-represented in its training data and produce interpretable, debuggable code. The agent is not inherently restricted to classical methods: prompting it to use a specific technique (learned visual features, neural controllers, Kalman filtering) would likely cause it to adopt that approach instead. The choice of technique is a prompt-level decision, and more modern perception or control methods could be introduced simply by instructing the agent to use them. Exploring this prompt-steerable technique selection is a direct avenue for future work.

**Future directions:** (i) Prompting the agent to use modern perception methods (e.g. learned keypoint detectors or foundation-model visual features) in place of hand-coded HSV segmentation, to improve robustness to lighting variation and novel objects. (ii) Combining AOR with a VLA prior for warm-started adaptation. (iii) Using Reflective Test-Time Planning [10] for sub-goal selection while AOR handles low-level implementation adaptation. (iv) Real-robot deployment with appropriate uncertainty modelling. (v) Theoretical characterisation of when in-context policy improvement converges, in terms of observability and reproducibility of failure modes.

## 9. Conclusion

This paper presented Act–Observe–Rewrite, a framework for in-context policy learning in robot manipulation that makes executable Python controller code the unit of LLM reasoning. The framework advances beyond prior work in verbal reflection (Reflexion, Reflective Test-Time Planning) by operating at the level of *motor-control implementation* rather than strategy description or sub-goal selection, and beyond prior work in robot code generation (Code as Policies, ProgPrompt) by closing the feedback loop with visual episode evidence.

On Lift and PickPlaceCan, AOR converges to 100%: the agent finds and corrects systematic failures—vision biases, in-

correct colour identification, centroid contamination by scene markers, coordinate convention errors—through iterative diagnosis and code rewriting. On Stack, it reaches 91% and stalls. Every residual failure involves gripper contact with cubeB during placement; the agent observed this in episode images and correctly named it as the cause. It did not, however, find a controller variant that avoids the contact, despite such variants likely existing. This is an honest result: the reflexion search converged to a local optimum and did not recover.

Collectively, these results establish that multimodal coding agents occupy a distinct, practically useful position in the robot learning design space: no demonstrations, no reward engineering, no gradient updates—yet high task-specific performance, full interpretability, and a systematic approach to understanding *why* a controller fails. As foundation models become more capable reasoners about geometry and physics, we expect this combination of verbal diagnosis and code synthesis to become an increasingly important tool for deploying physical AI systems in the real world.

## References

- [1] M. Ahn, A. Brohan, N. Brown, et al. Do as I can, not as I say: Grounding language in robotic affordances. In *Conference on Robot Learning (CoRL)*, 2022.
- [2] H. Bharadhwaj, J. Vakil, M. Sharma, A. Gupta, S. Tulsiani, and V. Kumar. RoboAgent: Generalization and efficiency in robot manipulation via semantic augmentations and action chunking. In *International Conference on Robotics and Automation (ICRA)*, 2024.
- [3] K. Black, N. Brown, D. Driess, et al.  $\pi_0$ : A vision-language-action flow model for general robot control, 2024. arXiv:2410.24164.
- [4] A. Brohan, N. Brown, et al. RT-2: Vision-language-action models transfer web knowledge to robotic control. In *Conference on Robot Learning (CoRL)*, 2023.
- [5] A. Chen, D. Dohan, and D. So. EvoPrompting: Language models for code-level neural architecture search. In *Advances in Neural Information Processing Systems (NeurIPS)*, 2024.
- [6] C. Chi, Z. Xu, S. Feng, et al. Diffusion policy: Visuomotor policy learning via action diffusion. In *Robotics: Science and Systems (RSS)*, 2023.
- [7] D. Driess, F. Xia, M. S. M. Sajjadi, et al. PaLM-E: An embodied multimodal language model. In *International Conference on Machine Learning (ICML)*, 2023.
- [8] Y. Feng, J. Han, Z. Yang, X. Yue, S. Levine, and J. Luo. Reflective planning: Vision-language models for multi-stage long-horizon robotic manipulation. In *Conference on Robot Learning (CoRL)*, 2025.
- [9] D. Ghosh, H. Walke, K. Pertsch, K. Black, O. Mees, S. Dasari, J. Hejna, T. Kreiman, C. Xu, J. Luo, et al. Octo: An open-source generalist robot policy. In *Robotics: Science and Systems (RSS)*, 2024.
- [10] Y. Hong, H. Huang, M. Li, F.-F. Li, J. Wu, and Y. Choi. Learning from trials and errors: Reflective test-time planning for embodied LLMs, 2024. Stanford University and Northwestern University. <https://reflective-test-time-planning.github.io/>.
- [11] W. Huang, F. Xia, T. Xiao, et al. Inner monologue: Embodied reasoning through planning with language models. In *Conference on Robot Learning (CoRL)*, 2022.
- [12] W. Huang, C. Wang, R. Zhang, Y. Li, J. Wu, and L. Fei-Fei. ReKep: Spatio-temporal reasoning of relational keypoint constraints for robotic manipulation, 2024. arXiv:2409.01652.
- [13] T. Kagaya et al. Memory transfer planning: LLM-driven context-aware code adaptation for robot manipulation, 2025. arXiv:2509.24160.
- [14] M. J. Kim, K. Pertsch, S. Karamcheti, et al. OpenVLA: An open-source vision-language-action model. In *Conference on Robot Learning (CoRL)*, 2024.
- [15] J. Liang, W. Huang, F. Xia, P. Xu, K. Hausman, B. Ichter, P. Florence, and A. Zeng. Code as policies: Language model programs for embodied control. In *International Conference on Robotics and Automation (ICRA)*, 2023.
- [16] Y. J. Ma, W. Liang, G. Wang, D.-A. Huang, O. Bastani, D. Jayaraman, Y. Zhu, L. Fan, and A. Anandkumar. Eureka: Human-level reward design via coding large language models. In *International Conference on Learning Representations (ICLR)*, 2024.
- [17] Y. J. Ma, W. Liang, G. Wang, et al. DrEureka: Language model guided sim-to-real transfer. In *Robotics: Science and Systems (RSS)*, 2024.
- [18] A. Madaan, N. Tandon, P. Gupta, S. Hallinan, L. Gao, S. Wiegrefe, U. Alon, N. Dziri, S. Prabhunoye, Y. Yang, S. Gupta, B. P. Majumder, K. Hermann, S. Welleck, A. Yazdanbakhsh, and P. Clark. Self-refine: Iterative refinement with self-feedback. In *Advances in Neural Information Processing Systems (NeurIPS)*, 2023.
- [19] NVIDIA et al. GR00T N1: An open foundation model for generalist humanoid robots, 2025. arXiv:2503.14734.
- [20] Open X-Embodiment Collaboration. Open X-Embodiment: Robotic learning datasets and RT-X models. In *Conference on Robot Learning (CoRL)*, 2023.

- [21] K. Rana, J. Haviland, S. Garg, J. Sherrat, N. Suenderhauf, and F. Dayoub. SayPlan: Grounding large language models using 3d scene graphs for scalable robot task planning. In *Conference on Robot Learning (CoRL)*, 2023.
- [22] S. Reed, K. Zolna, et al. A generalist agent. *Transactions on Machine Learning Research (TMLR)*, 2022.
- [23] B. Romera-Paredes, M. Barekatin, A. Novikov, M. Balog, M. P. Kumar, E. Dupont, F. J. R. Ruiz, J. S. Ellenberg, P. Wang, O. Fawzi, P. Kohli, and A. Fawzi. Mathematical discoveries from program search with large language models. *Nature*, 626, 2024.
- [24] N. Shinn, F. Cassano, A. Gopinath, K. Narasimhan, and S. Yao. Reflexion: Language agents with verbal reinforcement learning. In *Advances in Neural Information Processing Systems (NeurIPS)*, 2023.
- [25] I. Singh, V. Blukis, A. Mousavian, A. Goyal, D. Xu, J. Tremblay, D. Fox, J. Thomason, and A. Garg. Prog-Prompt: Generating situated robot task plans using large language models. In *International Conference on Robotics and Automation (ICRA)*, 2023.
- [26] H. Sun, Y. Zhuang, L. Kong, B. Dai, and C. Zhang. Ada-Planner: Adaptive planning from feedback with language models. In *Advances in Neural Information Processing Systems (NeurIPS)*, 2023.
- [27] V. Vosylius and E. Johns. Instant policy: In-context imitation learning via graph diffusion. In *International Conference on Learning Representations (ICLR)*, 2025.
- [28] N. Wake, A. Kanehira, K. Sasabuchi, J. Takamatsu, and K. Ikeuchi. GPT-4V(ision) for robotics: Multimodal task planning from human demonstration. *IEEE Robotics and Automation Letters (RA-L)*, 2024.
- [29] G. Wang, Y. Xie, Y. Jiang, A. Mandlekar, C. Xiao, Y. Zhu, L. Fan, and A. Anandkumar. Voyager: An open-ended embodied agent with large language models. *Transactions on Machine Learning Research (TMLR)*, 2023.
- [30] C. Yang, X. Wang, Y. Lu, H. Liu, Q. V. Le, D. Zhou, and X. Chen. Large language models as optimizers. *arXiv preprint arXiv:2309.03409*, 2024.
- [31] K. Yang, D. Klein, A. Celikyilmaz, N. Peng, and Y. Tian. RLCD: Reinforcement learning from contrast distillation for language model alignment. In *International Conference on Learning Representations (ICLR)*, 2024.
- [32] S. Yao, J. Zhao, D. Yu, N. Du, I. Shafraan, K. Narasimhan, and Y. Cao. ReAct: Synergizing reasoning and acting in language models. In *International Conference on Learning Representations (ICLR)*, 2023.
- [33] W. Yu, N. Gileadi, C. Fu, S. Kirmani, K.-H. Lee, M. G. Arenas, H.-T. L. Chiang, T. Erez, L. Hasenclever, J. Humplik, B. Ichter, T. Xiao, P. Xu, A. Zeng, T. Zhang, N. Heess, S. Levine, K. Hausman, and Y. Tassa. Language to rewards for robotic skill synthesis. In *Conference on Robot Learning (CoRL)*, 2023.
- [34] T. Z. Zhao, V. Kumar, S. Levine, and C. Finn. Learning fine-grained bimanual manipulation with low-cost hardware. In *Robotics: Science and Systems (RSS)*, 2023.

## A. Agent Reasoning: Examples and Failure Cases

This appendix presents verbatim excerpts from the agent’s between-episode reasoning, illustrating both strong and weak diagnostic behaviour.

### Example 1: Correct vision-bias diagnosis (Lift, episode 0)

After episode 0, all key frames showed the arm hovering at a fixed position while the cube sat 8–9 cm below. The phase log showed zero phase transitions over 500 steps. The agent’s response:

**Diagnosis:** [ ```misalignment```, ```vision_bias``` ]

**Reasoning:** “The arm reached a hover position approximately 8–9 cm from the cube and remained there for 500 steps without ever entering the descend phase. The phase transition requires  $|\Delta xy| < 0.02$  m and  $|\Delta z| < 0.02$  m. Looking at the key frames, the arm appears to hover consistently to the upper-left of the cube’s actual position—suggesting a systematic offset in the `object_pos` estimate, likely from depth sensor bias. This is not a gain issue—no amount of gain tuning will help if the target position itself is wrong.”

**Strategy:** “Add a 2.5 cm depth correction offset (subtract from estimated `z` to compensate for depth sensor surface bias). Also relax the `reach`→`descend` threshold from 0.02 m to 0.035 m `xy` to handle estimation noise.”

**Confidence:** 0.72

This diagnosis was correct. The key distinguishing evidence was visual: the arm’s position was *stable* across all frames—it had converged to a wrong position, not failed to converge. The text-only metric `min_distance = 0.087` is ambiguous between “close but can’t converge” and “targeting a wrong position”; the images resolve this.

### Example 2: Vision pipeline bug isolated after 6 failed iterations (Stack, iteration 6)

After six controller versions all produced the same ~6 cm systematic placement miss to the right, the agent produced:

**Diagnosis:** [ ```vision_pipeline_error```, ```back_projection_bug``` ]

**Reasoning:** “Six iterations of controller changes have produced zero improvement in placement accuracy. The error magnitude (5–8 cm) is constant across all controller versions—this rules out gain tuning, phase threshold adjustments, and timing changes as fixes. A 5–8 cm systematic error that is invariant to controller logic is almost certainly a vision pipeline calibration issue. The depth camera in `robosuite` uses OpenGL row-major convention where row 0 is the *bottom* of the image. The standard back-projection formula assumes row 0 is the top. If the `y`-coordinate is not flipped during back-projection, the

resulting 3D position is reflected about the image centre—producing a systematic error proportional to the vertical pixel offset. `cubeB` sits below the image centre, so the unflipped estimate places it above the true position, which in 3D world coordinates corresponds to the observed consistent rightward miss.”

**Strategy:** “Do not change the controller logic. Audit the back-projection formula: use `img_height - 1 - pixel_row` not `pixel_row`. Also verify that the extrinsic matrix convention matches the renderer: `robosuite` uses OpenGL for rendering but the provided extrinsic uses an OpenCV axis correction incompatible with OpenGL images.”

**Controller code:** (no controller change requested—pipeline fix first)

**Confidence:** 0.85

Both bugs were confirmed in `src/vision.py`. Correcting them reduced placement error from 5–8 cm to 1.4–1.9 cm and enabled the subsequent controller iterations to reach 70% and ultimately 91%. This example illustrates the key capability: the agent used the *convergence argument* (six iterations, invariant error) and *visual spatial reasoning* (direction and magnitude of miss) to localise a bug to a specific line of pipeline code, without any human inspection.

### Example 3: Agent failure — retry with the same approach (Stack, iteration 17)

After the grasp-retry mechanism was added in v17, the agent detected that the retry was firing (frame count rose from 27–29 to 32–39) but not improving success. The diagnosis was:

**Diagnosis:** [ ```grasp_miss```, ```retry_ineffective``` ]

**Reasoning:** “The retry mechanism is triggering on approximately 20% of episodes and successfully re-approaching the cube. However, the retry uses the same `x_correction = -0.015` as the initial attempt, which means it is approaching from the same angle and depth as the first attempt. If the first attempt misses due to a specific geometric configuration (e.g. cube near the edge of the vision field, slight angle bias), the second attempt will reproduce the same miss. Adding a small variation to `x_correction` on retry should help.”

**Strategy:** “Vary `x_correction` on each retry: attempt 0 uses `x_corr = -0.015` (standard), attempt 1 uses `x_corr = 0.000` (centred approach).”

**Confidence:** 0.65

The strategy was conceptually correct but introduced a **bug**: the single `self.x_correction` parameter was used for *both* the `cubeA` grasp approach *and* the `cubeB` placement alignment. Changing it on retry caused the placement target to shift by 1.5 cm, creating placement failures that masked the improvement in grasp success. The result (v18) measured 76% vs. an expected ~85%.

The agent diagnosed the bug after seeing v18’s results, noting that placement failures (reward  $\sim 75$ –200) had increased while hard grasp failures decreased—a pattern consistent with the target having moved. The fix (v19) separated `x_corr_A` (varied per retry) from `x_corr_B` (fixed at  $-0.015$  for cubeB alignment), restoring placement accuracy and achieving 83%.

### ***Where the agent does not do well***

Three systematic weaknesses emerged across the iteration sequence:

**Bug introduction during refactoring.** The v18 case above is the clearest example: a conceptually sound change (vary approach angle on retry) was implemented by modifying a shared parameter, inadvertently breaking placement. The agent does not “simulate” the effect of code changes on all phases—it reasons locally about the change it intends to make and misses side-effects on other uses of the same variable.

**Stochastic vs. systematic confusion.** In early Stack iterations, the agent repeatedly proposed threshold tightening and gain changes to improve grasp reliability. Many of these changes were neutral or slightly harmful because the grasp failures were stochastic (dependent on exact initial cube placement) rather than systematic. The agent required multiple iterations of observing the same failure mode with different controller parameters before concluding that controller changes were not the solution. A more efficient agent would distinguish stochastic variance from systematic bias earlier, for example by correlating failures with initial-state randomness across episodes.

**Confidence miscalibration.** The agent’s `confidence` field frequently did not predict whether the proposed change would improve performance. High-confidence diagnoses (0.8+) sometimes led to regressions (v17: 6/10, below the 8/10 baseline), while low-confidence changes (0.5–0.6) sometimes produced the largest improvements (v16 retract ramp). The confidence field captures the agent’s subjective certainty about the diagnosis but not its effect size or potential for side-effects.